International Journal of Civil Engineering

Soil Mechanics Classic

Active earth pressure induced by strip loads on a backfill

O. Farzaneh[1], F. Askari[2,*], J. Fatemi[1]

Received: July 2013, Revised: October 2013, Accepted: November 2013

Abstract

Presented is a method of two-dimensional analysis of the active earth pressure due to simultaneous effect of both soil weight and surcharge of strip foundation. The study's aim is to provide a rigorous solution to the problem in the framework of upper-bound theorem of limit analysis method in order to produce some design charts for calculating the lateral active earth pressure of backfill when loaded by a strip foundation. A kinematically admissible collapse mechanism consisting of several rigid blocks with translational movement is considered in which energy dissipation takes place along planar velocity discontinuities. Comparing the lateral earth forces given by the present analysis with those of other researchers, it is shown that the results of present analysis are higher (better) than other researchers' results. It was found that with the increase in $q/\gamma H$, the proportion of the strip load (q) which is transmitted to the wall decreases. Moreover, Increasing the friction between soil and wall (δ) will result in the increase of effective distance (d_e). Finally, these results are presented in the form of dimensionless design charts relating the mechanical characteristics of the soil, strip load conditions and active earth pressure.

Keywords: *Retaining wall, Active lateral earth pressure, Limit analysis, Upper-bound, Strip load.*

1. Introduction

Recent studies of retaining walls include experimental studies, numerical analysis and analytical models [1-3]. The evaluation of lateral earth pressure in retaining walls is of great interest in geotechnical engineering projects. Although active earth pressure against retaining structures has received much attention, the evaluation of active earth pressure of backfill when loaded by a strip foundation, has been slightly studied. This problem is generally treated using two different approaches: (a) two-step approach; in this approach the active earth force in absence of strip load is calculated using classical earth pressure methods, then added to strip load-generated force obtained from elastic or approximate methods [4]. (b) direct approach; in this approach the active earth force is calculated due to simultaneous effect of both the soil weight and the surcharge of strip load. Limit equilibrium method and limit analysis method (current research) are in this category.

There are some classic methods to calculate the active earth force in absence of strip load. Coulomb [5] first proposed a method in which the solution of the earth pressure problem was obtained analytically by considering a failure wedge and imposing the force equilibrium conditions. Rankine [6] successfully proposed another solution which is basically the same as Coulomb's method, developed in stress terms. Mueller Breslau [7] also obtained an analytical solution for the active earth pressure taking into account the slope of backfill and the soil-wall friction.

Two approximate methods for calculating the strip load-generated lateral force have also been proposed by Blum [8] and Cernia [9]. The earth pressure distributions obtained with these methods differ significantly from each other and may lead to either very conservative or unsafe solutions [10].

Jarquio [11] and Misra [12] provided solutions for lateral stresses on the wall due to the strip load based on Boussinesq's elastic half space solution.

Steenfelt and Hansen [13], Motta [14] and Greco [4] extended Coulomb approach, in which the evaluation of active earth force when a strip load acts, is obtained by limit equilibrium method.

Jarquio [11] concludes that Boussinesq's elastic-based solution for lateral stresses on a completely rigid wall is general solution applicable to both yielding and unyielding retaining wall structures but Steenfelt and Hansen [13] recommend Boussinesq solution only for unyielding structures, and that for the active state retaining walls the coulomb approach would be more reasonable.

Kim and Barker [15] evaluated lateral earth pressure due to live load surcharge in retaining walls and bridge abutments. They also provided approaches to obtain a simplified pressure distribution and calibration procedure

** Corresponding author: askari@iiees.ac.ir*
1 School of Civil Engineering, Faculty of Engineerin/g, University of Tehran, Shanzdah Azar Avenue, Enghelab Street, P.O. Box: 14155-6457, Tehran, Iran
2 No 21,IIEES, West Arghavan St, North Dibaji St, Farmanieh, P.O.Box: 3913/19395, Tehran, Iran

for the traditional method. Esmaeili and Fatollahzadeh [16] calculated the lateral pressure on the bridge abutments induced by the operational railway live load pattern LM71 using elasticity-based equations. Greco [17-18] presented an analytical solution to assess active thrust and its point of application due to line load surcharge based on coulomb's approach. Ghanbari and Taheri [19] also proposed analytical methods to calculate lateral pressure caused by a line surcharge on retaining walls with and without reinforcement. They modified horizontal slice method (HSM) and obtained a new formulation of this work to determine the effect of a line surcharge on conventional and reinforced retaining walls with frictional or cohesive-frictional backfills.

Caltabiano et al. [20] proposed a new solution to calculate the yield acceleration and the inclination of the failure surface in a surcharged backfill based on the pseudo-static equilibrium of the soil-wall system. They also investigated the effect of intensity of the surcharge and of its distance from the wall. Mojallal et al. [21] obtained the coefficient of yield acceleration and permanent displacements of geosynthetic-reinforced walls with full-height rigid panel facing (GRS-FHR walls) using the upper-bound theorem of limit analysis.

Yildiz [22] have studied the lateral earth force and its point of application due to strip loads by using an artificial neural network solution based on the data obtained from nonlinear finite element method. There are also a large number of research works which have been

This paper pertains to the solution of the active earth pressure by the upper-bound theorem of limit analysis when a strip of vertical load exists on the backfill which is, in fact, a development of the methods proposed for slope stability and earth pressure problems in primary works [23-25].

Approximate Methods

There are two approximate methods to calculate the strip load-generated lateral earth force. These methods are presented in Figs. 1(a and b). Cernia [9] proposed 45° distribution approach, which the effect of strip load q is considered as a 45 degree angle distribution at the depth of a. In the Beton Kalendar [26] approach (Fig. 1(b)), which was originally presented by Blum [8], the effect of strip load can be applied as either a triangular or uniform distribution on the wall.

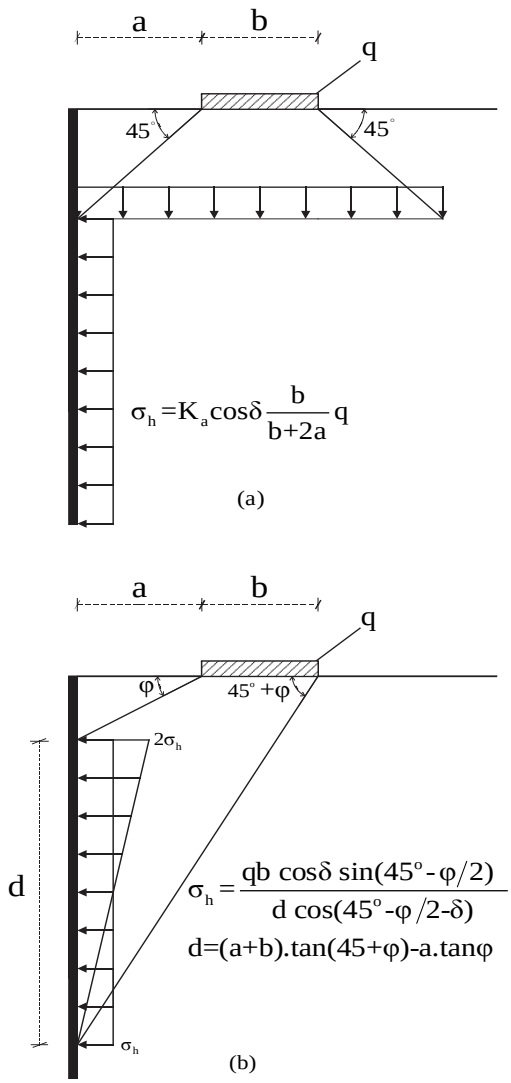

Fig. 1 Approximate approaches: (a) 45 degree distribution[9]; (b) Beton Kalender distribution [8, 26]

Elastic Method

Jarquio [11] presented a solution based on Boussinesq's elastic half space solution for lateral stresses on a rigid wall (Fig. 2). The use of elastic solution for lateral force due to surcharges is arguable and this approach has some defects. First, it is illogical that the strip load contributes to the lateral pressure at the top of the wall even when it is at some distance from the wall. This assumption leads to an unreasonably high position of the point of application of the total lateral force. Second, this solution is independent of the state of failure (active or passive) and the values of ϕ and δ[13].

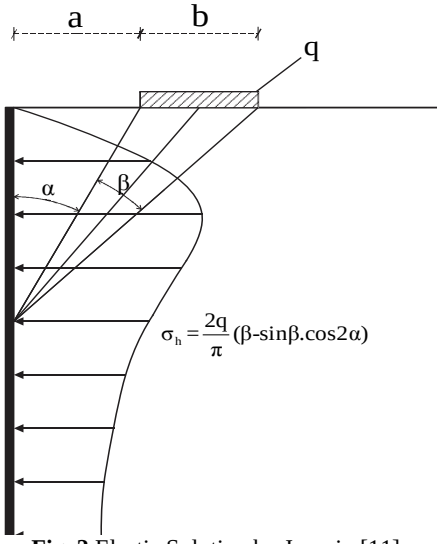

Fig. 2 Elastic Solution by Jarquio [11]

Limit Equilibrium Method

Steenfelt and Hansen [13], Motta [14] and Greco [4] obtained lateral earth forces due to the soil weight and the strip load using the wedge equilibrium analysis, which is, in fact, an extension of the conventional Coulomb active earth pressure analysis. This approach is shown in Fig. 3.

The approach used in this paper is based on upper-bound theorem of limit analysis method and can be used to determine active lateral force due to simultaneous effect of both the soil weight and the surcharge of strip load.

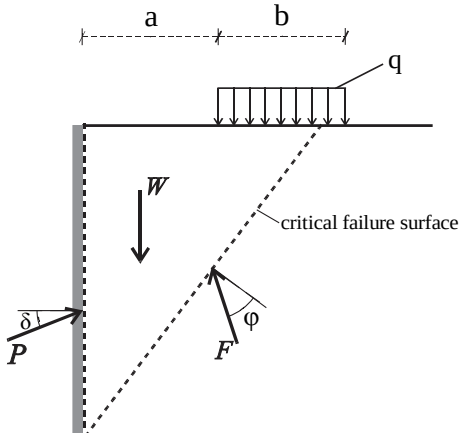

Fig. 3 Limit Equilibrium Method [4,13,14]

2. Upper- and Lower-Bound Theorems of Limit Analysis

The limit theorems of limit analysis method can be used to determine upper- and lower-bound solutions for the stability and limit load problems.

These theorems are explicit extension of the principle of maximum work derived by Hill [27], and were given in the form of theorems by Drucker, Greenberg and Prager [28]. The assumptions made in this method are: (a) the material is perfectly plastic at the limit state; (b) the limit state is defined by a yield function $f(\sigma_{ij}) = 0$, which is convex in the stress space; (c) the material obeys the associated flow rule (normality condition)

$$\dot{\varepsilon}_{ij}^{p} = \dot{\lambda}\,\frac{\partial f(\sigma_{ij})}{\partial \sigma_{ij}} \tag{1}$$

Where $\dot{\varepsilon}_{ij}^{p}$=plastic strain rate tensor of the soil; σ_{ij}=stress tensor; and $\dot{\lambda}$=non-negative multiplier that is positive when plastic deformations occur.

The lower-bound theorem states that, if a statically admissible stress field is found, then the load obtained from such stress field is smaller than or equal to the true limit load. Such admissible stress field is one that satisfies statical boundary conditions and equations of statical equilibrium at every point of the material and does not violate the yield function of the material.

The upper-bound theorem can be stated as: if a kinematically admissible velocity field is found, then the load obtained from such field, through the balance of external forces work and internal dissipation, is not lower than the true limit load. The kinematically admissible velocity field is one that complies with the kinematical boundary conditions and compatibility conditions following the flow rule [Eq. (1)].

Equating the rate of external work to the rate of internal energy dissipation for a kinematically admissible velocity field gives an unsafe solution of the collapse or limit load, but since the direction of the lateral force acting on the wall is opposite to the displacement direction of the wall, the upper-bound analysis yields the lower bound to the true value of the active lateral force. This concept will be shown as the lateral force acting on the wall is determined by an optimization procedure.

3. Assumed Failure Mechanism

Figure 4(a) shows the cross-section of the assumed collapse mechanism. It is composed of several rigid translational motion blocks separated by planar velocity discontinuity surfaces. The energy dissipation takes place only at the interfaces between adjacent blocks that constitute velocity discontinuities. The assumed mechanism starts from behind the strip foundation and continues to reach the surface of the wall either in the middle of the wall or in the heel of the wall.

The formulation can be extended to any number of blocks without any extra analytical calculation. The

movement of the wall is assumed to be horizontal. This horizontal movement of the wall is accommodated by the movement of the rigid blocks. The strip foundation is assumed to be completely rough in a way that no relative movement between soil and the foundation is allowed. Thus, the velocity vectors of the block No. n-1 and the strip foundation are the same.

As shown in Fig. 4(a), block No. 0 is adjacent to the vertical wall and is limited by the lower plane *FE* and the radial plane *OE*. Block No. i is bounded by two radial planes *OD* and *OC*, the lower plane *DC* and the ground surface *OM*. Block No. n-1 emerges from ground surface where the strip foundation is located.

Due to the normality condition, the velocity increment vectors across velocity discontinuity surfaces are inclined to those surfaces at the internal friction angle ϕ. As shown in Figs. 4(b and c), the velocities V_i of the blocks ($i = 0,1,2,\dots,n-1$; n=the number of blocks) and the velocity discontinuities between adjacent blocks $[V]_i$ can be derived by means of trigonometry in the way that the velocity V_F, which is vertical component of velocity vector of the block No. n-1, is considered to be unit ($V_F = 1$), then other velocities and velocity discontinuities are calculated from hodograph.

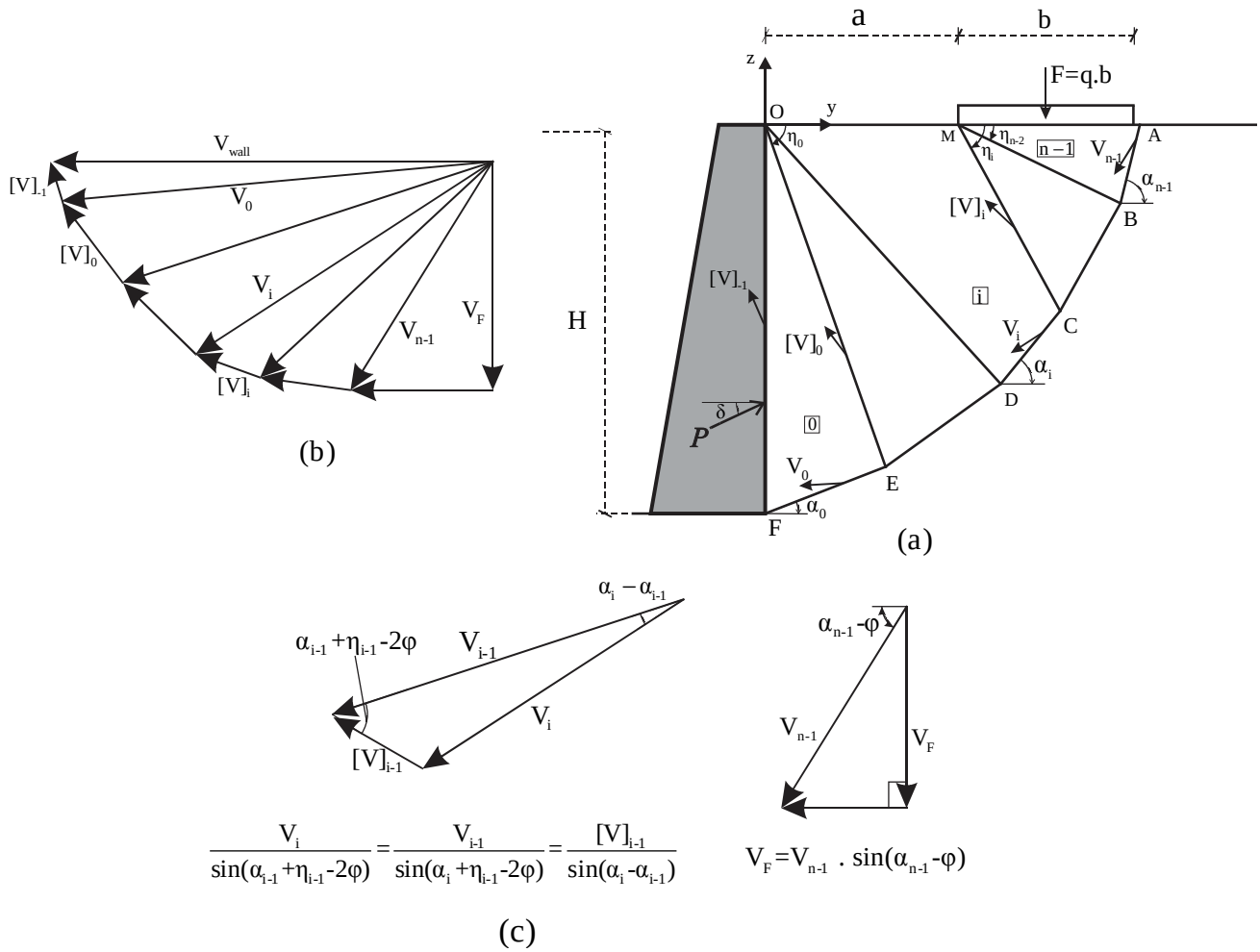

Fig. 4 Collapse mechanism: (a) cross section; (b) hodograph; (c) trigonometric relationships between velocity vectors

Energy Balance Equation

The upper-bound theorem of limit analysis allows one to determine the upper bound to the work rate of unknown limit force rather than the upper bound to the limit force itself. The upper-bound theorem can be written in the form

$$\int_s V_i T_i dS + \int_v X_i V_i^u dv \le \int_v \sigma_{ij}^u \dot{\varepsilon}_{ij}^u \, dv \qquad (2)$$

Where the left-hand side of the inequality denotes the external rate of work and the right-hand side shows the work dissipation rate or internal rate of work. In this inequality T_i=unknown true limit stress vector on boundary S where velocity vector is V_i and v is the volume. The second term on the left-hand side denotes the work rate of body forces where X_i=body force vector; and V_i^u=velocity vector. The term on the right-hand side of inequality denotes the rate of work dissipation within the material where $\dot{\varepsilon}_{ij}^u$= assumed field of admissible deformation rate; and σ_{ij}^u=stress field related to $\dot{\varepsilon}_{ij}^u$ through the flow rule [Eq. (1)].

The external rate of work includes works done by the active earth force P_a , the soil weight of blocks and the

strip load q on the ground surface. The total rate of external work can be written as

$$\dot{Ex} = \dot{W}_{P_a} + \dot{W}_q + \dot{W}_{soil} \quad (3)$$

Where

$$\dot{W}_{soil} = \gamma \sum_{i=0}^{n-1} A_i \cos(\alpha_i - \phi)\, V_i \quad (4)$$

$$\dot{W}_q = q.b.1.V_{n-1}.sin(\alpha_{n-1} - \varphi) = q.b.1.V_F = q.b.1 \quad (5)$$

$$\dot{W}_{P_a} = -P_a \cos(\phi + \delta - \alpha_0)\, V_0 \quad (6)$$

Where A_i= area of block i; V_i= velocity of block i; V_{n-1}=velocity of the last block beneath the loaded area; V_0= velocity of first block adjacent to the wall; and b=width of the loaded area.

Velocity discontinuities, where energy dissipation takes place, consist of lower planes between the soil at rest and the soil in motion, radial planes separating the rigid blocks, and the soil-wall interface where soil-wall cohesion is considered to be $c' = c(tan\delta/tan\phi)$[24], so the total rate of internal energy dissipation can be written as

$$\dot{Int} = c\cos\phi \left[\sum_{i=0}^{n-1} A_{L_i}.V_i + \sum_{i=0}^{n-2} A_{R_i}.[V]_i\right] + c\left(\frac{tan\delta}{tan\phi}\right).H.\sin(\alpha_0 - \phi)V_0 \quad (7)$$

Where A_{L_i}=area of lower plane i for unit length of the wall; and A_{R_i}= area of radial plane i for unit length of the wall.

For assumed rigid-block mechanism, the inequality (2) can be written as

$$\dot{W}_{P_a} + \dot{W}_q + \dot{W}_{soil} \le \dot{Int} \quad (8)$$

By replacing the equations (4),(5),(6) and (7) in inequality (8), one can write it as follows

$$-P_a \cos(\phi + \delta - \alpha_0)\, V_0 + q.b.1 \le c\cos\phi \left[\sum_{i=0}^{n-1} A_{L_i}.V_i + \sum_{i=0}^{n-2} A_{R_i}.[V]_i\right] + c\left(\frac{tan\delta}{tan\phi}\right).H.\sin(\alpha_0 - \phi)\, V_0 - \gamma \sum_{i=0}^{n-1} Ar_i \cos(\alpha_i - \phi)\, V_i \quad (9)$$

By extending aforementioned inequality, one can reach the following inequality

$$P_a \ge F(\alpha,\eta,\phi,\delta).\gamma H^2 + G(\alpha,\eta,\phi,\delta).qH - R(\alpha,\eta,\phi,\delta).cH \quad (10)$$

Where F,G and R are the functions of geometrical parameters (α,η) and soil properties (ϕ,δ). These dimensionless functions are defined as follows:

$$F = \frac{\sum_{i=0}^{n-1} Ar_i \cos(\alpha_i - \phi)\, V_i}{\cos(\phi + \delta - \alpha_0)\, V_0.H^2} \quad (11)$$

$$G = \frac{b}{\cos(\phi + \delta - \alpha_0)\, V_0.H} \quad (12)$$

$$R = \frac{\cos\phi \left[\sum_{i=0}^{n-1} A_{L_i}.V_i + \sum_{i=0}^{n-2} A_{R_i}.[V]_i\right] + \left(\frac{tan\delta}{tan\phi}\right).H.\sin(\alpha_0 - \phi)V_0}{\cos(\phi + \delta - \alpha_0)\, V_0.H} \quad (13)$$

Optimization Procedure

For different mechanisms the right-hand side of inequality (10) is calculated. As it is obvious from inequality (10), the best answer is the one that is the maximum of these values. Therefore, the most critical active forces can be calculated by an optimization procedure (maximization) of P_a with respect to geometrical parameters (α,η) defining different mechanisms of failure. The optimization method used here is exactly the same procedure used by Farzaneh & Askari [25]. The optimization procedure includes two stages, first with initial assumed values of α_i and η_i the initial mechanism of failure is defined then the limit load is calculated. In the second stage, the values of α_i are changed simultaneously. The process of changing the values of α_i continues until no change in the limit load is observed. This procedure is also used to optimize the values of η_i .

4. Comparison with Existing Methods

Figure 5 shows the ratio $P/b.q$ (P is the lateral force due to the soil weight and the strip load) as the function of a/H obtained by existing methods and the present solution. As it is seen, for the strip loads which are too close to the wall (i.e., a/H smaller than 0.1) the 45° distribution approach gives larger estimations than the present solution. It can be explained in the way that in this method, the effect of strip loads when they are too close to the wall, are considered as a widespread surcharge acting on the slight depths behind the wall. For a/H greater than 0.1, the 45° distribution and the Beton Kalendar approaches underestimate the lateral earth force comparing to the current analysis. When a/H is greater than 0.5, the elastic solution presents higher predictions than the present method, however a rule-of-thumb is that strip load will have slight effect on lateral force if it is farther than the height away from the wall.

Figures 6 and 7 illustrate a comparison between the current method and the limit equilibrium method (extended Coulomb approach). In Fig. 6, $P/b.q$ is plotted versus internal friction angle, ϕ. As it can be seen, the results of the current method are higher (better) than the limit equilibrium method. This improvement is about 3% on average.

Figure 7 provides another comparison between two approaches. In this Figure, ratio $P/b.q$ obtained for different distances of the strip load from the wall (a/H) is shown. In both analyses, lateral earth force decreases

significantly as the strip load distance increases. The results of the present method are higher (better) than limit equilibrium method. This improvement, when $a/H = 0.5$, attains 8% and 16% for $q/\gamma.H = 1$ and $q/\gamma.H = 2$, respectively.

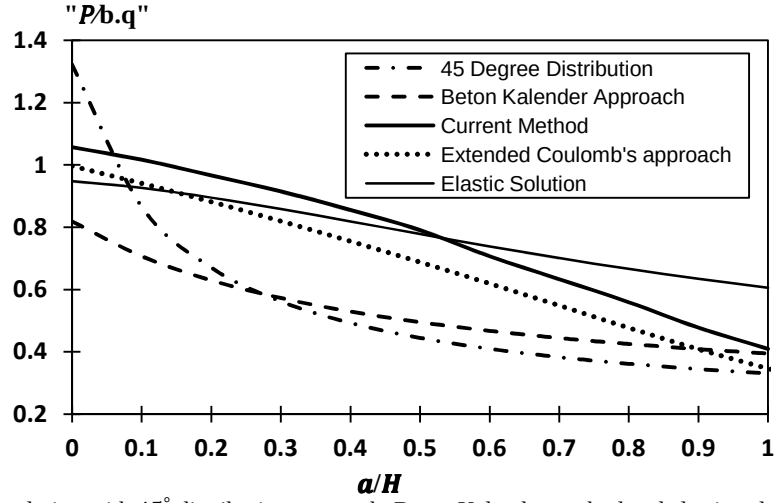

Fig. 5 Comparison of present solution with 45° distribution approach, Beton Kalendar method and elastic solution for: $\phi = 30°$, $b/H = 0.3$, $\delta/\phi = 2/3$, $q/\gamma H = 1.5$

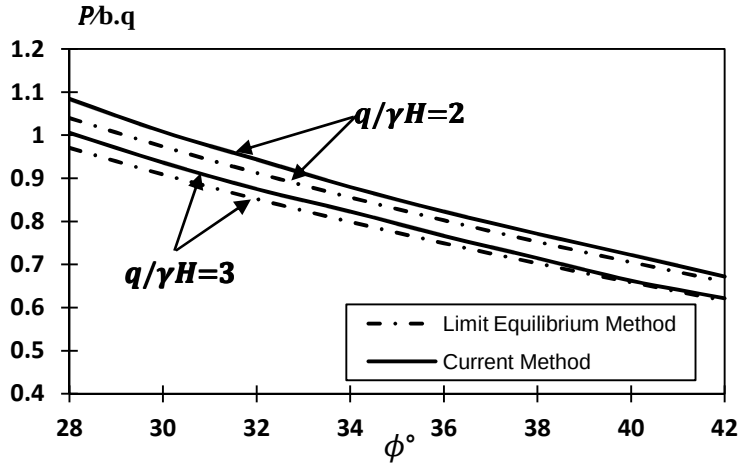

Fig. 6 Comparison of current method with extended Coulomb approach for: $a/H = 0$, $b/H = 0.3$, $\delta/\phi = 1/2$

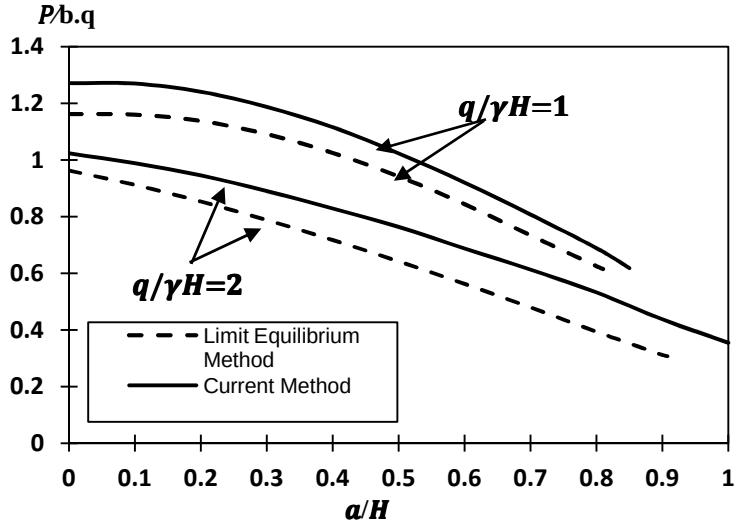

Fig. 7 Comparison of current method with extended Coulomb approach for: $\phi = 35°$, $b/H = 0.2$, $\delta/\phi = 1/2$

Table 1 shows a comparison for lateral force induced by a line load between current method and those proposed by Motta [14] and Ghanbari and Taheri [19]. As it can be seen, there is a good agreement between analyses. In addition, solution proposed by Ghanbari and Taheri [19] gives higher values when $d = 2m$ (d= distance of line load from the wall) in relation to two other methods, whereas for $d = 4m$ current method and Motta's approach present higher values compared to Ghanbari and Taheri's solution. However, the maximum difference between present method and two other methods is about 8 %.

Table 1 Comparison of active earth force between present method, Motta [14] and Ghanbari and Taheri [19]:

$\phi = 30^\circ, c = 0kPa, \gamma = 20\,kN/m^3, \delta = 10^\circ, H = 10m$

Active earth force(kN/m)				
ϕ=30°		Current Method	Motta [14]	Ghanbari and Taheri [19]
q(kN/m)	d(m)			
20	2	319	324	322
	4	319	319	315
50	2	337	347	344
	4	335	335	322
100	2	370	359	380
	4	366	362	335

5. Numerical Results

The mechanisms and formulations proposed in this research can be used to determine the total lateral force acting on the wall due to the soil weight and the strip load.

A failure mechanism (Fig. 8) consisting of six rigid blocks is used to determine the total lateral force due to the soil weight and the surcharge of strip load. Changing the position of the strip load, a series of charts was obtained.

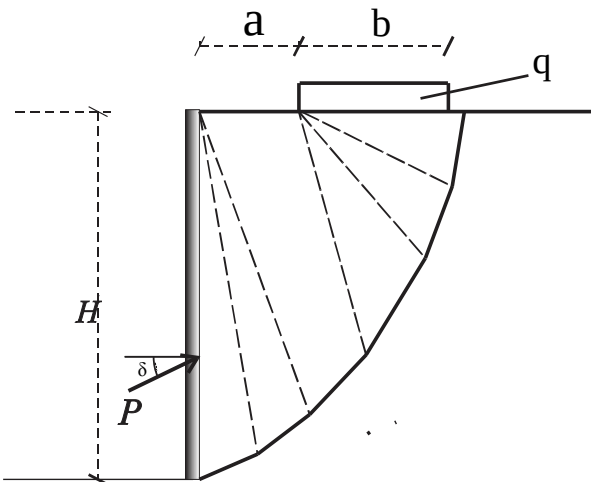

Fig. 8 Failure mechanism used in lateral earth force analyses

Figures 9, 10, 11 and 12 provide the ratio of the total lateral force (P) to $b.q$ for various condtions of the problem. Parameters presented here are: $P/b.q$, $q/\gamma.H$, a/H , b/H , d_e/H , δ/ϕ , ϕ. d_e is the effective distance beyond which the strip load does not affect the lateral active earth. This distance corresponds to the last point in the charts. Other parameters are shown in Fig. 4.

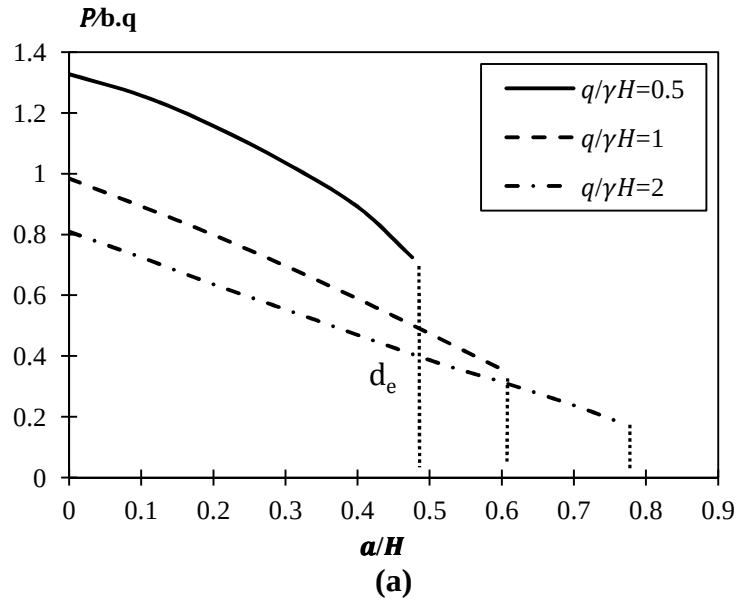

(a)

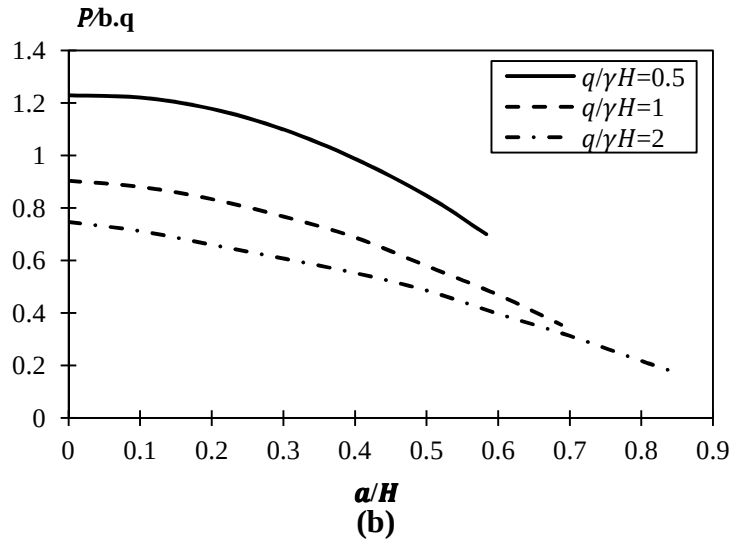

(b)

Fig. 9 Design charts for lateral earth force due to simultaneous effect of the soil weight and the strip load with: $\phi = 40°$, $b/H = 0.3$; (a) $\delta/\phi = 0$; (b) $\delta/\phi = 1$

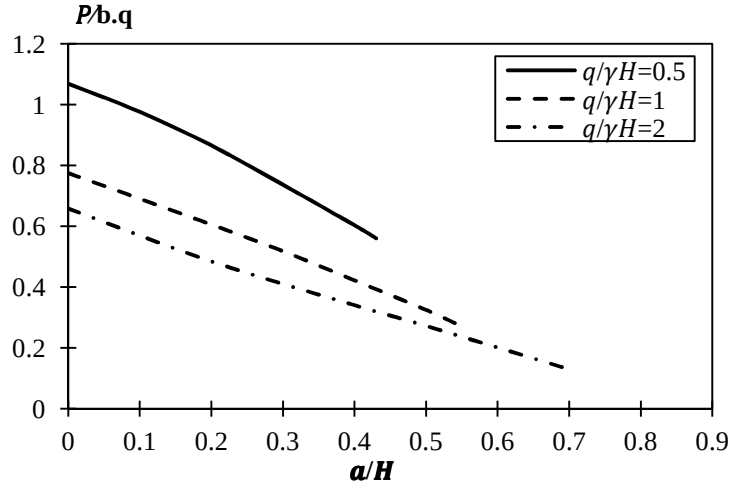

(a)

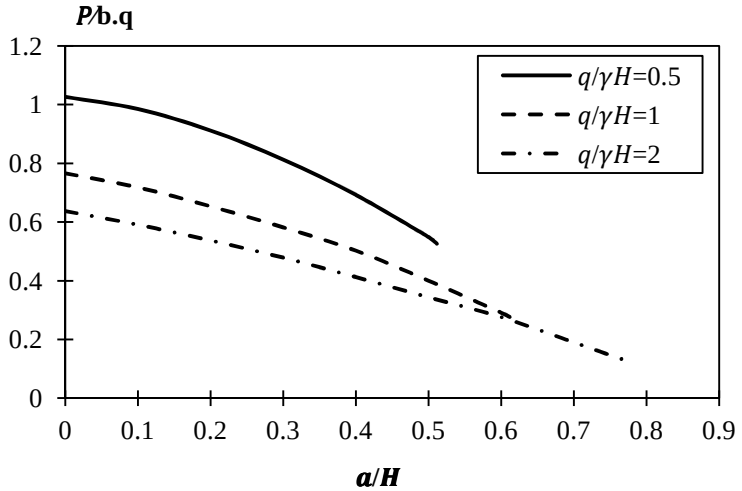

(b)

Fig. 10 Design charts for lateral earth force due to simultaneous effect of the soil weight and the strip load with: $\phi = 40°$, $b/H = 0.4$; (a) $\delta/\phi = 0$; (b) $\delta/\phi = 1$

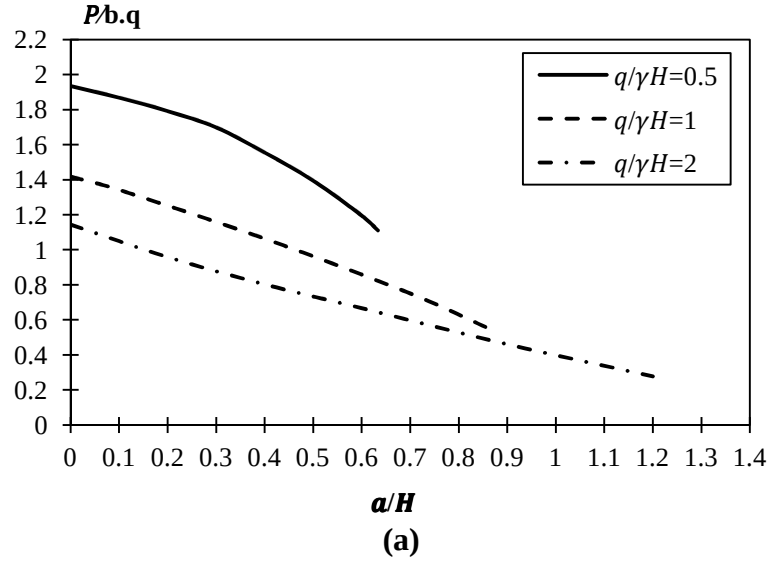

(a)

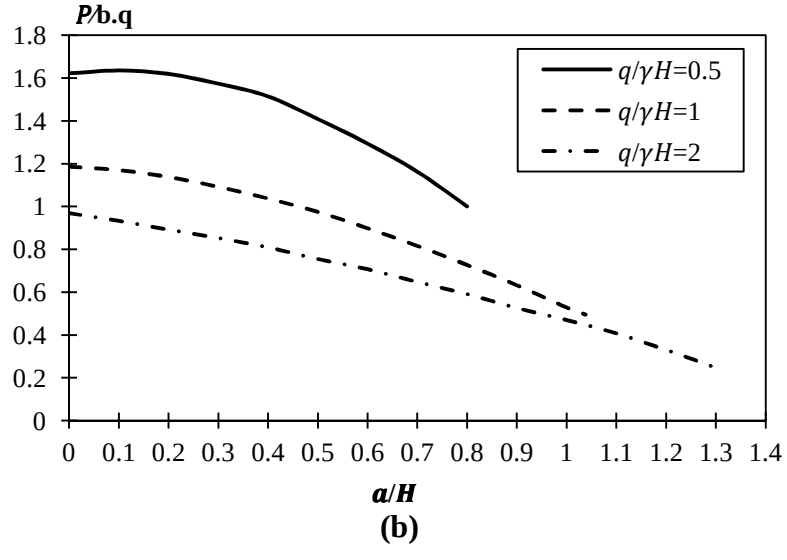

(b)

Fig. 11 Design charts for lateral earth force due to simultaneous effect of the soil weight and the strip load with: $\phi = 30°$, $b/H = 0.3$; (a) $\delta/\phi = 0$; (b) $\delta/\phi = 1$

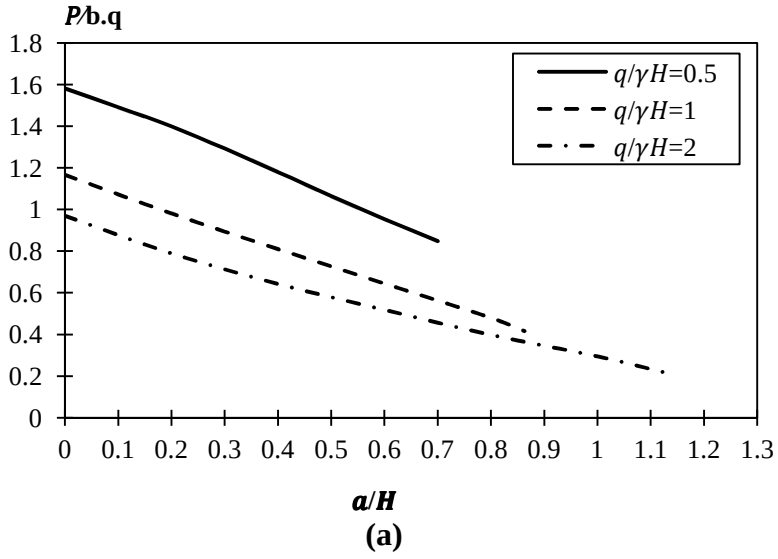

(a)

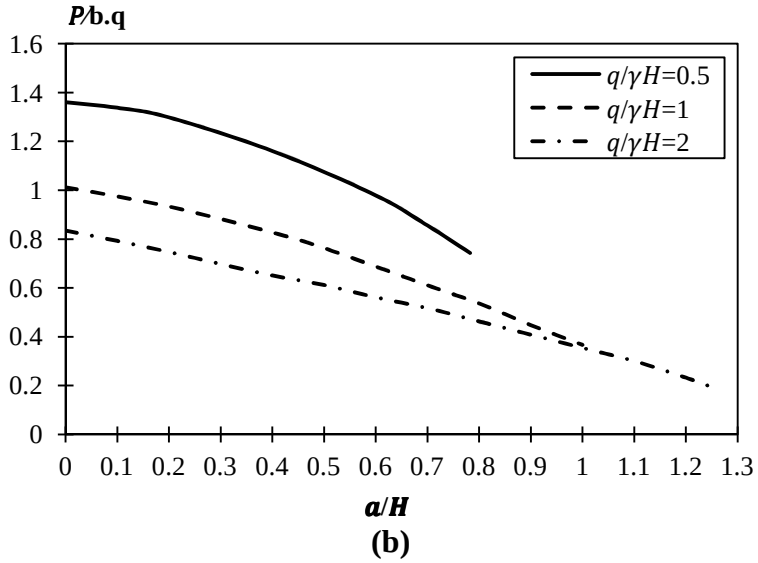

(b)

Fig. 12 Design charts for lateral earth force due to simultaneous effect of the soil weight and the strip load with: $\phi = 30°$, $b/H = 0.4$; (a) $\delta/\phi = 0$; (b) $\delta/\phi = 1$

The influence of the position of the strip load (a/H) and the strip load intensity ($q/\gamma H$) can be easily derived from these charts as follows:

- The ratio $P/b.q$ decreases with the growth of $q/\gamma H$. This states that the proportion of the strip load which is transmitted to the wall decreases with the growth of the strip load intensity ($q/\gamma H$). For instance, for configurations $\phi = 30°, \delta/\phi = 1, b/H = 0.3, a/H = 0.4$, when $q/\gamma H$ equals to 1, the proportion of the strip load (q) which is transmitted to the wall is 31% while, when $q/\gamma H$ equals to 2 this percentage is 24%.
- Increasing the distance between the wall and the strip load, the total lateral force decreases significantly.
- Generally, the higher ratio $q/\gamma H$ is, the higher the critical distance d_e. for example, for $\phi = 30°$, $\delta/\phi = 1, b/H = 0.3$, the effective distance corresponding to $q/\gamma H = 2$, is 20% greater than the effective distance pertained to $q/\gamma H = 1$.
- Decreasing the friction angle of the soil, the effective distance drastically increases. For instance, for configurations $q/\gamma H = 2$, $b/H = 0.4, \delta/\phi = 1$, the effective distance (d_e) corresponding to $\phi = 30°$ is 39% greater than the effective distance corresponding to $\phi = 40°$.
- With the increase in friction angle between soil and wall, the effective distance increases. For example, for $\phi = 30°$, $q/\gamma H = 2, b/H = 0.3$, the effective distance pertained to $\delta/\phi = 1$ is 8% greater than the effective distance pertained to $\delta/\phi = 0$.

6. Conclusion

This paper has presented a formulation based on upper-bound approach of limit analysis for evaluation of active earth force when a strip foundation acts on the backfill. The analysis allows assessment of active earth force with various strip load conditions and soil properties. The collapse mechanism consists of several rigid blocks with translational movement which is a development of the method proposed by Farzaneh and Askari [25].

Comparing the present analysis with the conventional Coulomb method proposed by Steenfelt and Hansen [13], Motta [14] and Greco [4] and also method presented by Ghanbari and Taheri [19], it indicates good compatibility. The results are presented in the form of dimensionless charts. The main conclusions based on these results can be obtained as follows:

1. With the increase in $q/\gamma H$, the proportion of the strip load (q) which is transmitted to the wall decreases.
2. Decreasing the friction angle of the soil, the effective distance drastically increases.
3. Increasing the friction between soil and wall, the effective distance increases.

Notation

The following symbols are used in this paper:

a	=	distance of the strip load from the wall
A_i	=	area of block i
A_{L_i}	=	area of lower plane i for unit length of the wall
A_{R_i}	=	area of radial plane i for unit length of the wall
b	=	loading width
c	=	cohesion of soil
d_e	=	effective distance
H	=	wall height
i	=	block number
n	=	total number of blocks
$P\ or\ P_a$	=	active earth force due to soil weight and the strip load
q	=	strip load intensity
S	=	boundary
T_i	=	true limit stress vector
v	=	Volume

V_i	=	velocity of block i
$[V]_i$	=	velocity jump between blocks
X_i	=	body force vector
α_i , η_i	=	geometrical parameters of failure mechanism
γ	=	specific weight of soil
δ	=	friction angle between soil and wall
$\dot{\varepsilon}_{ij}$	=	stress rate tensor
σ_{ij}	=	stress tensor
ϕ	=	internal friction angle

References

[1] Ghanbari A, Hoomaan E, Mojallal M. An analytical method for calculating the natural frequency of retaining walls, International Journal of Civil Engineering, 2013, No. 1, Vol. 11, pp. 1-9.

[2] Ghanbari A, Ahmadabadi M. Active earth pressure on inclined retaining walls in static and seismic conditions, International Journal of Civil Engineering, 2010, No. 2, Vol. 8, pp. 159-173.

[3] Kaveh A, Shakouri Mahmud Abadi A. Harmony search based algorithm for the optimum cost design of reinforced concrete cantilever retaining walls, International Journal of Civil Engineering, 2011, No. 1, Vol. 9, pp. 1-8.

[4] Greco VR. Lateral earth pressure due to backfill subject to a strip of surcharge, Geotechnical and Geological Engineering, 2006, Vol. 24, pp. 615-636.

[5] Coulomb CA. Sur une application des re `gles de maximis et minimis a ` quelques proble `mes de statique relatifs a `l'architecture, Me´moires de savants e´trangers de l'Acade´mie des Sciences de Paris, 1773, Vol. 7, pp. 343-382 (in French).

[6] Rankine WJM. On the mathematical theory of the stability of earthwork and masonry, Proceedings of Royal Society, 1857, Vol. 8.

[7] Mueller Breslau H. Erddruck auf Stu¨tzmauern, Kroener, Stuttgart, Germany, 1906, (in German).

[8] Blum H. Beitrag zur berechnung von bohlwerken unter beruchsichtigung der wandverformung, Verlag von Wilhelm Ernst and Sohn, Munich, Germany, 1951.

[9] Cernia JN. Geotechnical Engineering: foundation design, John Wiley & Sons, Inc, New York, 1995.

[10] Georgiadis M, Anagnostopoulos C. Lateral pressure on sheet pile walls due to strip load, Journal of Geotechnical and Geoenvironmental Engineering, 1998, No. 1, Vol. 124, pp. 95-98.

[11] Jarquio R. Total lateral surcharge pressure due to strip load, Journal of the Geotechnical Engineering Division, 1981, No. 10, Vol. 107, pp. 1424-1428.

[12] Misra B. Lateral pressures on retaining walls due to loads of surface of granular backfill, Soils Found, 1980, No. 2, Vol. 20, pp. 31-44.

[13] Steenfelt JS, Hansen B. Discussion of 'Total lateral surcharge pressure due to strip load,' by R. Jarquio, Journal of Geotechnical Engineering, 1983, No. 2, Vol. 109, pp. 271-273.

[14] Motta E. Generalized Coulomb active-earth pressure for distanced surcharge, Journal of Geotechnical Engineering, 1994, No. 6, Vol. 120, pp. 1072-1079.

[15] Kim J, Barker M. Effect of live load surcharge on retaining walls and abutments, Journal of Geotechnical and Geoenvironmental Engineering, 2002, No. 10, Vol. 128, pp. 808-813.

[16] Esmaeili M, Fatollahzadeh A. Effect of train live load on railway bridge abutments, Journal of Bridge Engineering, 2013, No. 4, Vol. 18, pp. 576-583.

[17] Greco VR. Active thrust due to backfill subject to lines of surcharge, Journal of Geotechnical and Geoenvironmental Engineering, 2006, No. 2, Vol. 132, pp. 269-271.

[18] Greco VR. Active earth thrust by backfills subject to a line surcharge, Canadian Geotechnical Journal, 2005, No. 5, Vol. 42, pp. 1255-1263.

[19] Ghanbari A, Taheri M. An analytical method for calculating active earth pressure in reinforced retaining walls subject to a line surcharge, Geotextiles and Geomembranes, 2012, Vol. 34, pp. 1-10.

[20] Caltabiano S, Cascone E, Maugeri M. Seismic stability of retaining walls with surcharge, Soil Dynamics and Earthquake Engineering, 2000, Nos. 5-8, Vol. 20, pp. 469-476.

[21] Mojallal M, Ghanbari A, Askari F. A new analytical method for calculating seismic displacements in reinforced retaining walls, Geosynthetics International, 2012, No. 3, Vol. 19, pp. 212-231.

[22] Yildiz E. Lateral pressures on rigid retaining walls: a neural network approach, MS thesis, The Middle East Technical University, Ankara, 2003.

[23] Michalowski, R. L., Three dimensional analysis of locally loaded slopes, Geotechnique, 1989; 391, 27–38.

[24] Soubra AH, Regenass P. Three-dimensional passive earth pressures by kinematical approach, Journal of Geotechnical and Geoenvironmental Engineering, 2000, No. 11, Vol. 126, pp. 969-78.

[25] Farzaneh O, Askari F. 3D analysis of nonhomogeneous slopes, Journal of Geotechnical and Geoenvironmental Engineering, 2003, Vol. 1292, pp. 137-145.

[26] Beton Kalender. Verlag von Wilhelm Ernst and Sohn, Munich, Germany, 1983.

[27] Hill R. A variational principle of maximum plastic work in classical plasticity, The Quarterly Journal of Mechanics and Applied Mathematics, 1948, Vol. 1, pp. 18-28.

[28] Drucker DC, Prager W, Greenberg HJ. Extended limit design theorems for continuous media, Quarterly of Applied Mathematics, 1952, Vol. 94, pp. 381-389.